Experimental investigation on the dynamic performance of a solar thermally-driven adsorption chiller integrated with a gas boiler

Elena Fuentes[1], Veronica Impala[1], Ivan Bellanco[1], Jaume Salom[1], Alejandra Sayans[2], Miquel Balsells[2], Silvia Sanjoaquín[2] and Oscar Mogro[3]

[1] Catalonia Institute for Energy Research, IREC, Barcelona (Spain)

[2] Naturgy, Barcelona (Spain)

[3] BDR Thermea Group, Barcelona (Spain)

Abstract

The present study investigates the dynamic performance of a state-of-the-art adsorption chiller to provide useful cooling for a residential and a tertiary building. The equipment was tested at a hardware-in-the-loop configuration in a laboratory setting under the dynamic loads of two simulated building models at two climatic zones in Spain. The adsorption chiller was connected to a hot tank of 760 L volume used to store the heat from an emulated solar collector array. In addition, a gas boiler was used as an auxiliary source of heat to the storage tank. Summertime dynamic experiments of 24 hours were performed at the two building and climate scenarios. The efficiency of the system was analysed in terms of coefficient of performance, coverage of cooling demand and primary energy savings with respect to a reference system.

Keywords: solar cooling, adsorption, gas boiler.

1. Introduction

In the last decades, a great effort has been made to improve cooling technologies based on renewable energy sources. The use of solar energy is one of the most interesting solutions for climatization applications and air conditioning, as availability of solar radiation and cooling loads is largely coincidental. Currently, the vast majority of the cooling demand in buildings is covered with the use of traditional heat pump systems. The disadvantage of these systems is that they use refrigerants that contribute to greenhouse emissions and that the increasing installed capacity of heat pumps leads to the overload of electric grids and consequent black-outs, especially during warm periods (Palomba et al., 2017). For solar cooling, efforts are made to improve the efficiency of conventional solar thermal cooling technologies based on adsorption and absorption. While existing technologies are increasingly modified to improve their performance, the development of methods for the efficient integration of solar renewable equipment in different types of buildings is one of the main research and development directions for solar building climatization systems (Ge et al., 2018).

Adsorption is a proven technology able to harness the potential of solar heat and low grade waste heat for producing useful cooling. Generally, this type of adsorption chiller can be driven with waste heat with temperatures as low as 55°C (Wuang et al., 2005). Adsorption machines are a promising technology for implementation in southern Europe, where a consistent source of solar energy is available during the warm season. However, there is a lack of studies aiming at optimizing the integration and analyzing the behavior of these systems when operating under dynamic conditions. In this study it is presented a laboratory experimental investigation on the performance of a 2-bed adsorption chiller of 10 kW nominal cooling capacity and a thermal nominal COP of 0.65, operated under the dynamic loads of virtual buildings at quasi-realistic conditions.

doi:10.18086/eurosun2018.04.26 Available at http://proceedings.ises.org

2. Methodology

2.1. System concept and case scenarios

The system under study consists of a virtual building that is conditioned by means of a solar cooling system comprising an adsorption machine coupled to an air heat rejection unit, a solar thermal array of 8 panels and a gas boiler. The aim of the adsorption chiller is to cover the cooling needs of either a virtual residential or a tertiary building provided with a fancoils cooling distribution system that works at a chilled water set point of 15°C.

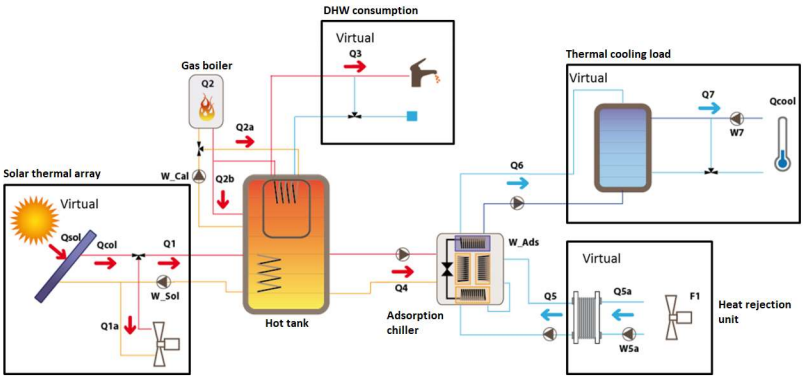

Fig. 1: Solar cooling system concept

The driving circuit of the adsorption machine was connected to a hot tank of 760 L used to store the heat from an emulated 8 collector solar thermal array and an auxiliary domestic gas boiler. The system was tested in a hard-ware-in the-loop configuration in which the adsorption chiller, the hot storage tank and the gas boiler were real laboratory components while the rest of the elements: solar array, cooling load and adsorption machine rejection unit were virtual components emulated by means of the laboratory thermal test benches according to the output from a simulation model (TRNSYS) that reproduced the behavior of the virtual systems (Fig. 1). The real and virtual components are listed in Tab. 2, along with the technical characteristics that were adopted using data from equipment technical datasheets.

Typical days of the summer were selected in order to test the performance of the system for two different climates in Spain and two different building scenarios: a single family dwelling and a small tertiary building (office). Statistical methods were applied for the selection of the case days, using typical climatic data of the geographic zones of interest. The days selected for the study are indicated in Tab. 1. The virtual building chosen for the climate of Salamanca (Mediterranean continental climate) is a single-family dwelling of 200 m^2 area and annual cooling demand of 15.6 kWh/m^2, while the scenario for Bilbao (oceanic climate) is an office building of 250 m^2 with an annual cooling demand of 7.5 kWh/m^2.

Tab. 1. : Scenarios considered for the summer day case studies

City (climate)	Building type	Day selected	Characteristic of selected day
Salamanca (Mediterranean continental)	Residential	21st July	Warmest day
		31st August	Lowest radiation day
		15th June	Average day
		22nd May	Average day
Bilbao (Oceanic)	Office	21st July	Warmest day
		10th August	Average day
		7th September	Lowest radiation day

Tab. 2. : Main technical characteristics of real and virtual components comprising the studied system

System	Type	Technical characteristics/model
Distribution system and cooling load	virtual	Cold water tank: 750 L (TRNSYS type 534) Fancoil system (TRNSYS type 682). Mixing valve (TRNSYS type 812) to control the supply water temperature to fancoils.
Solar array	virtual	8 solar panels, parallel arrangement Total aperture surface: 11.4 m^2; Flow rate: 30 l/h m^2 Optical efficiency: 0.817 Thermal loss coefficient: 3.716 W/m^2K Orientation: 40°
Heat rejection unit	virtual	Air rejection unit (TRNSYS type 511) Water nominal flow rate: 5.93 m^3/h Air nominal flow rate: 15005 m^3/h Electrical power consumption: 0.3 kW
DHW consumption	virtual	Tapping profiles as defined in standard EN 12976; cycles L, M Mains water temperature as defined in standard DBHE-2013
Adsorption chiller	real	Nominal COP:0.65; Nominal cooling capacity: 10 kW Cold water set point temperature: 14 °C
Gas boiler	real	Saunier-Duval Thema condens F25: thermal power 19.5 kW heating/25 kW DHW Baxi Platinum 24 AF: thermal power 24 kW heating/24 kW DHW
Hot storage tank	real	Tank-in-tank design 760 L volume

2.2. Experimental set up

The laboratory test benches are provided with a set of sensors and control loops that allow the monitoring and control of the temperature and water flow of the fluid circuits in the system. The temperatures are measured with PT100 type A sensors, calibrated in the working temperature range. The return temperatures from the solar array, the cooling load and the adsorption rejection system were emulated according to the output obtained from the simulation model by using individual heat exchangers through which secondary refrigeration and heating fluids are circulated for temperature control. In addition, for the control of the water flow and temperatures the test benches are equipped with two magnetic-inductive flow meters and two precision valves.

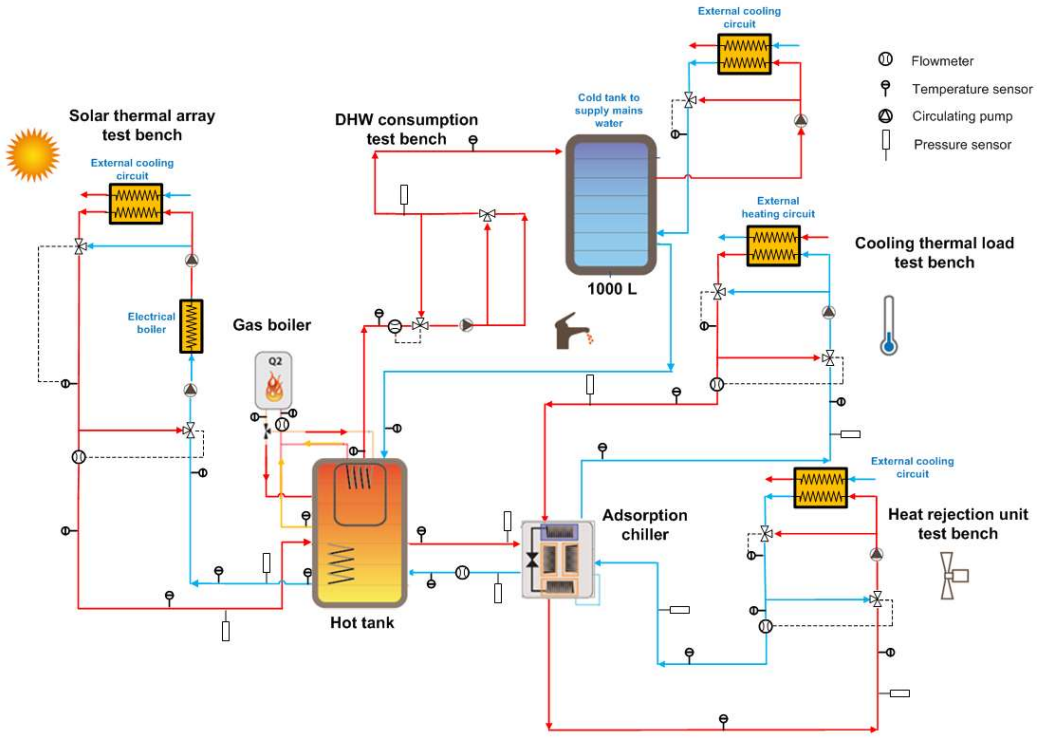

Fig. 2: Laboratory experimental set up

The gas consumption of the installation is measured at the gas inlet of the boiler with a digital flow meter. For reproducing the mains water temperature for DHW (domestic hot water), a 1000 L volume storage tank was used to store cold water that was conditioned according to the climate and period of the year under study.

Three series of experiments with a different control strategy for the auxiliary gas boiler were conducted, namely, set 1, 2 and 3. The control strategies were based on the operation of the gas boiler as a function of the hot tank temperatures (Tab. 3) at the exit tubing towards the boiler for heat production and at the immersed tank for DHW. The control strategies were sequentially proposed and tested in order to improve the results obtained from the previous control strategy evaluated, aiming at reducing the gas consumption while covering the cooling demand.

3.1. Performance of solar cooling system in different climates and typical days

In this section the behaviour of the components integrating the solar cooling system in different summer days is illustrated for the set of measurements corresponding to the first control strategy (set 1). For this control strategy the hot tank set point control temperature was set between 60-75 °C for heat production and 47 °C for DHW, while the set point temperature for the hot water produced by the boiler was 75 °C (Table 3). Fig.3 shows the evolution of the inlet and outlet temperatures of the solar collector circuit for the 4 selected days, Salamanca scenario. These results show that the days with the highest hot water temperature from the solar array are July 21st (day with highest outdoor temperatures) and June 15th (average day). The days with the lowest temperatures are the average day May 22nd and the day of lowest radiation, August 31st. Water circulation through the solar circuit activates from 10:30 am to 7:00 pm on the days with the highest temperatures, while for lower temperature days the solar circuit is active in a smaller time window, from approximately 11.00-12:00 to 17.00-18.00 h.

The activation of the adsorption chiller heat rejection unit is illustrated in Fig.4 in which the temperatures and the flow rate are shown. Very significant differences are observed regarding the time of activation and deactivation of the chiller among the different days under study. On July 21st the chiller starts at 8.45 am and stops at 11.30 am, with a shutdown interval between 11.30 am and 12.15 pm.

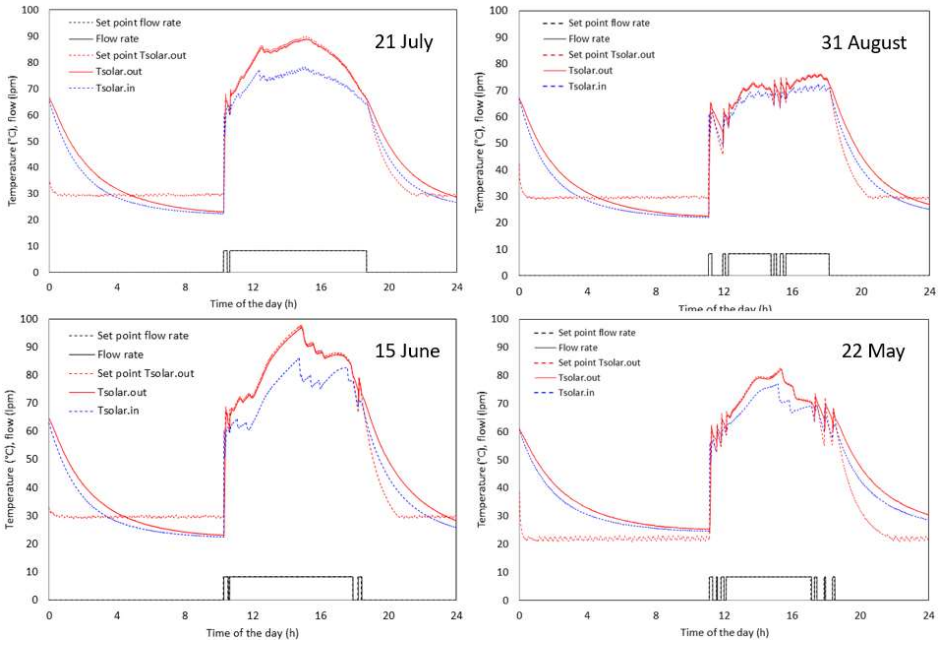

Fig.3 Comparison of solar array performance during different dynamic tests, Salamanca, set 1

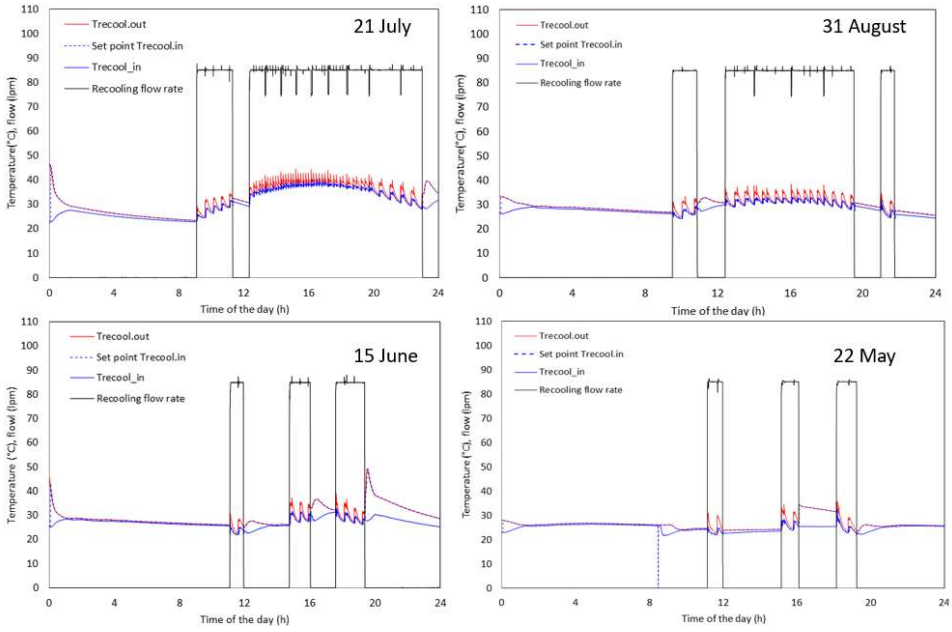

Fig.4 Comparison of recooling circuit (heat rejection unit) during different dynamic tests, Salamanca, set 1

For the warmest day, the inlet temperature to the chiller from the heat rejection unit is high, reaching values up to 37 °C. During the periods of high temperatures from the recooling circuit, the maximum cooling capacity achieved by the chiller is 4 kW. On the average days, June 15th and May 22nd, the machine is active for a shorter period of time, operating only during three intervals during the day and switching off before 8:00 pm. For the two average case days, the inlet temperature from the rejection unit is below 32 °C and a higher average cooling capacity of 7 kW is achieved. As most summer days will be represented by the average day, it is only on the extreme temperature days that the cooling capacity will be significantly reduced.

The effect of the external temperature on the cooling capacity is presented in Fig.5 where it is shown that during the periods of activation of the machine the temperature of the chilled water rises up to 22 °C for warmest day, while it remains below 18 °C and close to the 14 °C set point for the rest of the case days considered for Salamanca. The control strategy applied is able to maintain the hot water in the tank at a temperature above 60 °C in all cases

(Fig.6). However, the activation of the auxiliary boiler to keep these temperature levels is rather intensive for the highest temperature (21st July) and the lowest solar radiation (31st August) case days, while it is considerably lower for the average days.

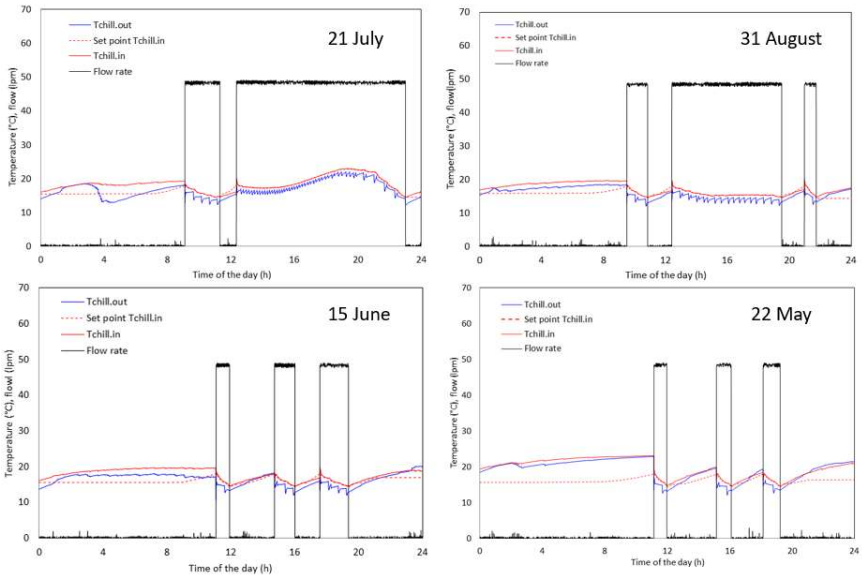

Fig.5 Comparison of cooling circuit during different dynamic tests, Salamanca, set 1

The ability of the solar cooling system to cover the cooling load for the Salamanca case with the control strategy 1 is illustrated in Fig.7, which shows the supply water temperature from the cold storage tank (T1) and the supply (T3) and return water temperatures (T2) of the fancoils distribution system. FR1 and FR2 are the water flows through the cold tank and the fancoils, respectively. The supply water to the fancoil (T3) is below 19 °C for all the scenarios but for the warmest case day (21st July). Considering a maximum supply temperature to the fancoils of 22 °C required to cover the cooling demand, it is not possible to fully cover the cooling needs on the warmest day.

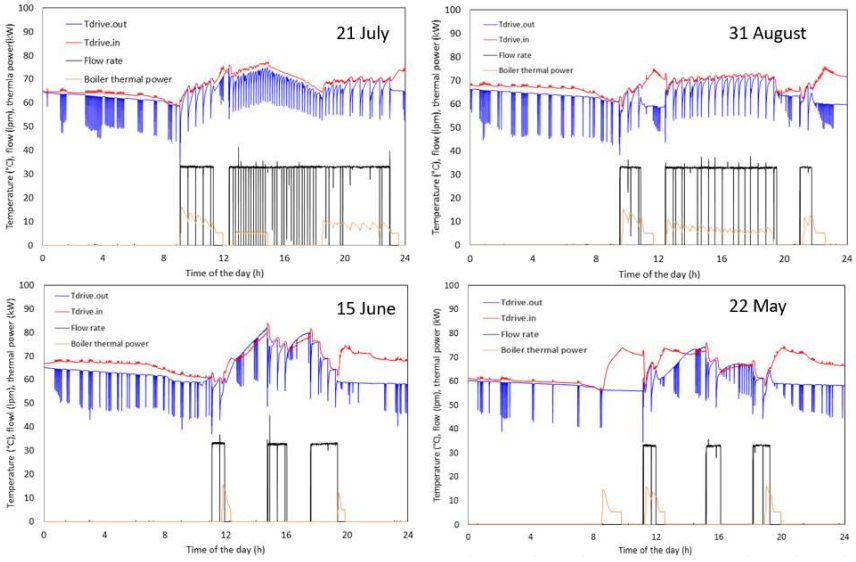

Fig.6 Comparison of driving circuit during different dynamic tests, Salamanca, set 1

The results indicate that the outdoor temperature is a dominant variable on the cooling load and the resulting performance of the system, since for Salamanca, both for the cloudiest and warmest day, an intensive activation of the boiler is needed to cover the cooling demand. When comparing with the Bilbao case (Fig. 8) the highest temperature case day (21st July) also exhibits the longest operation hours for the adsorption chiller (11 hours), as compared to the average and lowest radiation case days, in which the machine is activated between 3 and 4.4 hours

in the period of maximum external temperatures from 12-13 to 4 p.m. As in the case of Salamanca, the inlet temperature to the machine from the heat rejection unit reaches values up to 37 °C on the warmest day, whereas for the other case days this temperature remains below 32 °C during the whole period. Because of the lowest cooling capacity of the system on the warmest day, the temperature of the chilled water produced by the adsorption chiller rises up to 20 °C in the extreme temperature scenario, while it remains below 18 °C for the other case days.

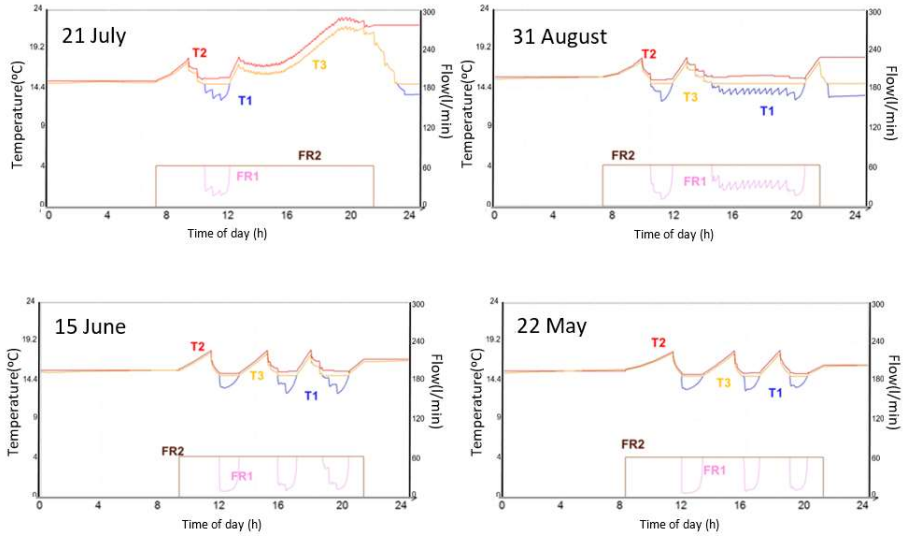

Fig.7 Comparison of distribution cooling system outlet temperature and flow profiles for different days, Salamanca, set 1.

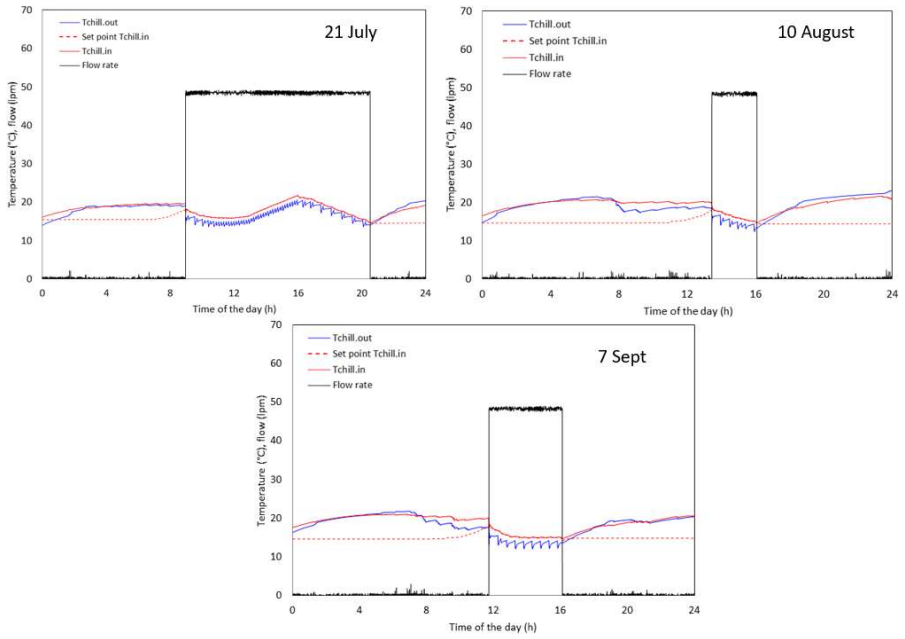

Fig. 8 Comparison of adsorption machine cooling circuit temperature and flow profiles for different days, Bilbao, set 1

In general, it is found that the daily activation of the boiler is mainly driven by the drop of the water tank temperatures that occurs when the chiller starts and it progressively returns cold water back into the tank. In the Bilbao scenario, similarly to the Salamanca case, the chiller is operative for long periods on the warmest day and it requires the support of the boiler to maintain the required temperatures in the hot tank (Fig.9). Regarding the influence of the cloudiness, it is seen that it is less influential than the temperature on the activation of the boiler, since on the cloudiest day (7th Sept) the auxiliary boiler is not needed to sustain the tank temperatures, whereas it operates intensively on the day with the highest cooling load (warmest day, 21st July).

Analogously to findings for Salamanca, the outlet temperature to the fancoils (Fig.10) in Bilbao is the highest for the warmest day, however it is still below the maximum temperature of 22 °C considered necessary to cover the

cooling demand. On the other hand, for the average and low radiation case days the temperature to the fancoils is considerably low, with a maximum value of 17 °C, thus fulfilling the requirements to cover the cooling load.

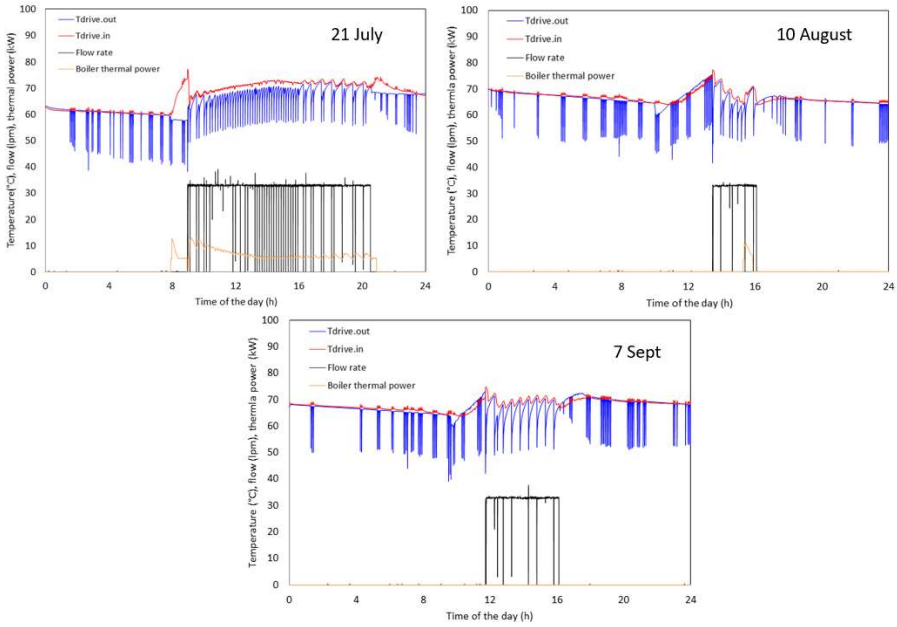

Fig.9 Comparison of driving circuit during different dynamic tests, Bilbao, set 1

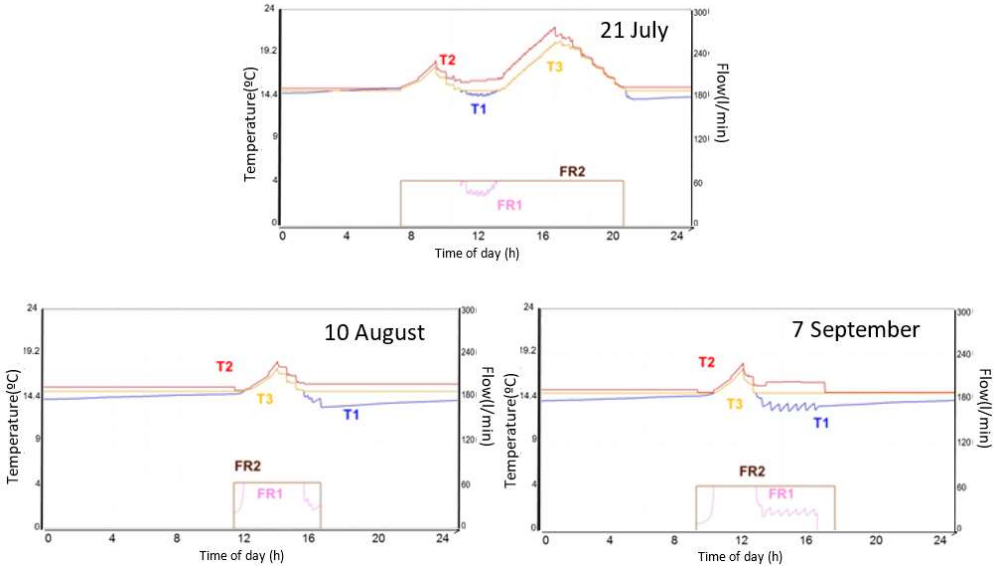

Fig.10 Comparison of distribution cooling system outlet temperature and flow profiles for different days, Bilbao, set 1

Significant operation differences for the adsorption chiller were obtained for the two climate and building scenarios studied (Fig.11). On the warmest case day, the chiller operated for at least 11 hours for both cases. Although the Salamanca scenario has higher temperatures and cooling load, the operating time for the boiler is 2.5 h longer on the warmest day for Bilbao, as this climate presents more cloudiness and lower solar radiation. For Salamanca, the operating times for the adsorption chiller and the gas consumption are 69-77% and 60-88% lower on an average day, respectively, than those in the warmest day. In the Bilbao scenario there is an even larger difference between the warmest and the average days. The operating hours of the chiller drop 77% from the warmest to the average case day, whereas the gas consumption drops a 94%.

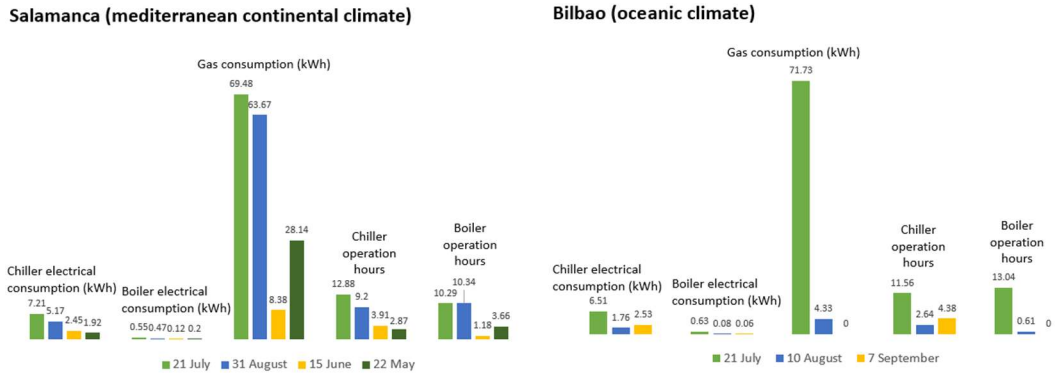

Fig.11 Comparison of daily electrical and gas energy consumption and number of operation hours for the gas boiler and adsorption chiller, Salamanca and Bilbao scenarios, set 1

The results shown in this section are for the first strategy (set 1) that was explorative and not optimized to cover the energy demand in all cases. Two more strategies (set 2 and set 3) were further proposed and applied sequentially in order to improve the system performance, aiming at covering the cooling demand while minimizing the auxiliary gas consumption. The performance results of the other two strategies applied is presented in the following section.

3.2. Performance of solar cooling system under different control strategies

Three control strategies were sequentially applied in order to optimize the performance of the solar cooling system to cover the cooling demand with a minimum of energy usage of the auxiliary gas boiler. In the different strategies applied, the boiler was started to reach a set point temperature in the hot tank (Tset_heating) by producing hot water with a set value (Tset_boi_heating). The control would also ensure that a set-point temperature (Tset_DHW) is maintained in the immersed tank of the storage in order to cover the DHW demand.

Tab. 3. : Summary of strategies tested for control of the gas boiler. Tset_heating: hot tank set point temperature, Tset_boi_heating: boiler set point outlet temperature for heating, Tset_DHW: immersed tank set point temperature, Tset_boi_DHW: boiler set point outlet temperature for DHW, Tamb: outdoor temperature, Tamb_max: maximum reference outdoor temperature used for control strategy.

Parameter	Tamb<20°C		20 °C< Tamb<Tamb_max °C	Tamb>Tamb_max °C
Tset_heating (°C)	Set 1	60 °C	Tamb+40, with Tamb_max=35 °C	75
	Set 2		2 Tamb+20, with Tamb_max=30 °C	80
	Set 3		1.5 Tamb+30, with Tamb_max=30 °C	75
Tset_boi_heating (°C)	Set 1	75	75	75
	Set 2	Minimum (82,Tset_heating+15)		
	Set 3			
Tset_DHW (°C)	Set 1	47.5	47.5	47.5
	Set 2			
	Set 3			
Tset_boi_DHW (°C)	Set 1	75	75	75
	Set 2			
	Set 3			

In addition, the boiler used in the first experiment series (set 1) was replaced by a different model. The boiler used in set 2 and 3 allows external modulating control of the output set point temperature while the first one was used with a fixed set point of 75 °C for both heating and DHW operation modes. Tab. 3 shows the different strategies (set 1, set 2 and set 3) used for operating the gas boiler as a function of the temperature in the hot storage tank. These strategies were tested on the warmest and average days of the two case scenarios under study in Salamanca and Bilbao, by performing laboratory experiments following the methodology described previously. The results of the strategies applied were evaluated with a number of indicators related to the energy performance and energy consumption of the system. The results were also compared with the energy usage from a reference system comprising a standard heat pump to cover the cooling demand and a gas boiler to cover the DHW needs.

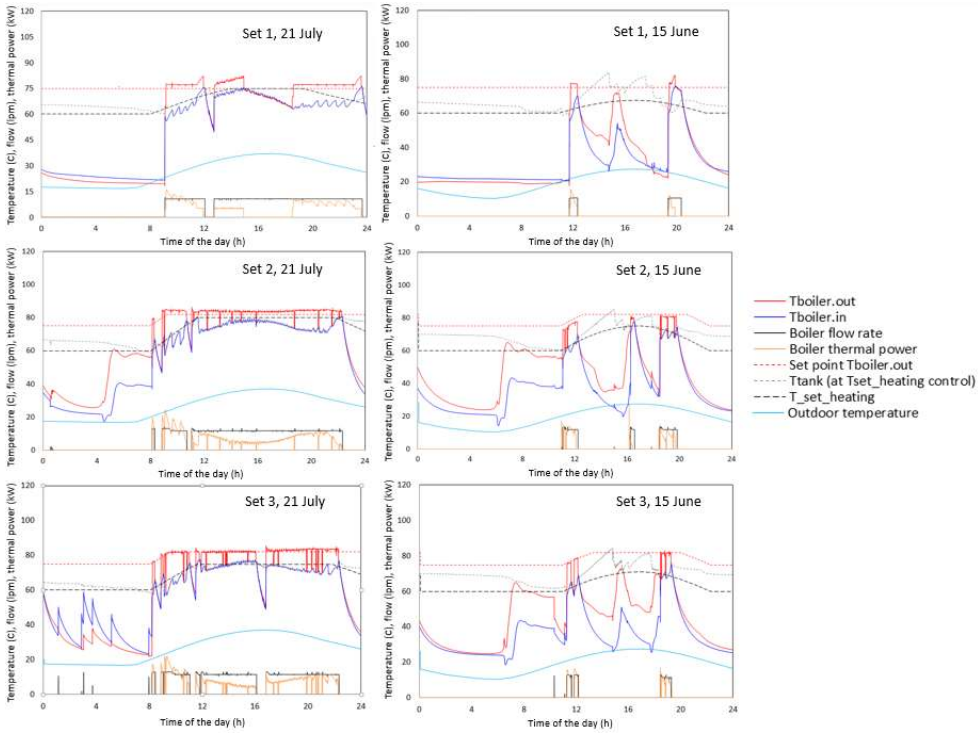

Fig.12 Comparison of gas boiler operation for the three control strategies applied (set 1, set 2 and set 3) on the warmest case day (21st July) and the average case day (15th June) , Salamanca scenario.

Fig.12 shows the operation of the boiler under the different strategies for the warmest and the average case days for the Salamanca scenario. The objective of all strategies is to maintain the temperature at the tank (Ttank_boiler) as close as possible to the set point (Tset_heating), which is defined as a function of the ambient temperature (Tamb). When the boiler is active, for the first strategy (set 1) a fixed set point output temperature of 75 °C is used. The first strategy used (set 1) was explorative and was not optimized to cover the energy demand in all cases. The application of this strategy on the warmest case day (A, set 1) results in a discontinuous operation of the gas boiler during the period of highest cooling demand with tank temperatures between 62 and 75 °C (Fig.12). The discontinuous operation of the boiler is due to an internal control operation that protects the system and prevents the boiler from starting until the temperatures have dropped below certain value. The result of using this control strategy is that the cooling load of the warmest day in Salamanca cannot be fully covered, although it is sufficient to cover the energy needs for the warmest day in Bilbao. For the Bilbao scenario, this strategy is suitable since this location has milder climate conditions than Salamanca.

Strategy 2 was next proposed as an improvement to strategy 1, with the aim of covering the cooling demand in all cases by using higher tank set point temperatures (Table 3). With the application of the second strategy (set 2) the temperatures in the tank are maintained above 65 °C for longer periods, since the boiler is active during most of the time that the chiller is operating. With this strategy, it is possible to cover the cooling demand in all scenarios at the expense of an increase in the gas consumption (Tab. 4), which leads to a reduction of primary energy savings

with respect to the reference system (reference to solar cooling system primary energy ratio), particularly for the average case day (Tab. 5). In order to achieve better energy savings for the average case days, strategy 3 (set 3) was further proposed as an improvement to strategy 2, to reduce the gas consumption while the load is still covered. For that, strategy 3 applies a moderate reduction of the set point tank temperatures with respect to those in set 2. Although when changing from strategy 2 to 3 no substantial change is seen on the warmest case day in terms of primary energy savings, a significant improvement is achieved for the average case days (Tab. 5), with an increase of 26-32 % in the primary energy savings ratio.

For set 3, the results show that the daily COP remains at a relatively high value between 0.52 and 0.63 during the average and the warmest days, while the primary energy savings ratio in the average day ranges from 0.67 to 0.85. The daily average COP values obtained are influenced by the inlet temperatures to the adsorption chiller. The inlet temperatures from the recooling and heat source circuits are higher for the warmest day with respect to the other days for both the Salamanca and Bilbao scenarios, which produces a lower COP than in the average days. When comparing the COP of the warmest day, Salamanca presents COP values that are slightly lower than in Bilbao, which can be due to the higher temperatures in the recooling circuit in the Salamanca warmest day with respect to the Bilbao case.

Although strategy 3 provides the best performance results it should be noted that there is a potential for improvement that could be achieved with alternate control strategies for the adsorption chiller as a function of the temperatures in the cold tank, with changes in the control settings of the gas boiler and by optimizing the solar collectors array configuration and panels number (Chekirou et al, 2016). Although the primary energy savings ratio of the solar cooling system in the summer yield values below 1, annual performance calculations considering both winter and summer periods leads to primary energy annual savings of the solar cooling system of 19% with respect to the reference system.

Tab. 4. : Summary of results obtained for the day with highest external temperatures (21st July) for Salamanca and Bilbao climate and building scenarios, under the 3 considered control strategies. Ref. indicates reference case. (Primary energy factors for Spain: 2.5 (electricity) and 1.1 (gas))

	Salamanca			Bilbao		
Parameter	**Set 1**	**Set 2**	**Set 3**	**Set 1**	**Set 2**	**Set 3**
Thermal COP	0.56	0.50	0.52	0.55	0.55	0.55
Collector efficiency	0.39	0.35	0.36	0.33	0.29	0.30
Boiler efficiency	1.03	1.01	0.98	1.07	1.00	0.98
Solar gain to driving heat + DHW energy ratio	0.37	0.29	0.30	0.28	0.25	0.25
Solar cooling electrical energy use (kWh)	13.74	12.23	12.92	12.5	10.81	12.21
Solar cooling gas thermal energy use (kWh)	78.16	103.5	101.2	80.69	97.46	101.0
Solar cooling primary energy use (kWh)	120.3	144.4	143.6	120.0	134.2	141.6
Ref. electrical energy use (kWh)	19.05	19.00	19.00	17.55	17.56	17.56
Ref. Gas thermal energy use (kWh)	4.4	4.4	4.4	1.7	1.7	1.7
Ref. Primary energy use, (kWh)	52.5	52.4	52.4	45.7	45.8	45.8
Reference to solar cooling primary energy ratio	-	0.36	0.36	0.38	0.34	0.32
Fraction of cooling load covered (%)	77	100	100	100	100	100
Fraction of DHW load covered (%)	100	100	100	100	100	100

Tab. 5. : Summary of results obtained for the average case day for Salamanca (15th June) and Bilbao (10th August) climate and building scenarios, under the 3 considered control strategies. Ref. indicates reference case.

	Salamanca			Bilbao		
Parameter	**Set 1**	**Set 2**	**Set 3**	**Set 1**	**Set 2**	**Set 3**
Thermal COP	0.62	0.52	0.63	0.62	0.60	0.63
Collector efficiency	0.36	0.34	0.35	0.31	0.29	0.29
Boiler efficiency	0.95	0.93	0.89	0.95	0.97	0.92
Solar gain to driving heat plus DHW energy ratio	0.96	0.75	0.97	1.06	0.95	1.01
System electrical energy usage (kWh)	4.79	4.94	4.63	3.22	3.21	3.24
System thermal energy, gas usage (kWh)	9.42	24.3	16.2	4.87	15.1	10.4
System primary energy usage (kWh)	22.30	39.09	29.34	13.40	24.66	19.58
Ref. electrical energy usage (kWh)	7.98	7.95	7.91	4.52	4.51	4.51
Ref. Thermal energy, gas usage (kWh)	4.7	4.7	4.7	1.66	1.70	1.70
Ref. Primary energy usage, (kWh)	25.1	25.0	25.0	13.11	13.15	13.15
Reference to solar cooling primary energy ratio	1.13	0.64	0.85	0.98	0.53	0.67
Fraction of cooling load covered (%)	100	100	100	100	100	100
Fraction of DHW load covered (%)	100	100	100	100	100	100

3. Summary and conclusions

The dynamic performance of a solar cooling system integrated with a gas boiler has been tested for two different buildings (residential and tertiary) and climate scenarios (continental mediterranean and oceanic) under a laboratory hardware-in-the-loop configuration. The system was tested on case days that represented average and extreme climate conditions, under different control strategies. The adsorption chiller was able to cover the cooling demand in all case days, with primary energy ratios between the solar cooling system and a reference system of 0.67-0.85. Although the energy savings for the solar cooling system in the summer are below 1, annual calculations considering both winter and summer yield primary energy annual savings of 19% with respect to the reference system. This energy savings could be further enhanced by increasing the number of solar panels to provide heat.

4. References

Ge, T.S., Wang, R.Z., Xu, Z.Y., Pan, Q.W., Du, S., Chen, X.M., Ma, T., Wu, X.N. , Sun, X.L., Chen, J.F., 2018. Solar heating and cooling: Present and future development. Renew. Energy, 126, 1126-1140.

Palomba, V., Vasta, S., Freni, A., Pan, Q.W., Wang, R.Z., Zhai, X., 2017. Increasing the share of renewables through adsorption solar cooling: a validated case study; Renew. Energy, 110, 126-140.

Wuang. X., Chua, H. T., Choon, Ng. K., 2005. Experimental Investigation of silica gel-water adsorption chillers with and without a passive heat recovery scheme. Int. J. Refrig., 28, 756-765.

Chekirou, W., Boukheit, N., Karaali, A., 2016. Performance improvement of adsorption solar cooling system. Int. J. Hydrogen Energ. 41, 7169-7174.